

Repulsive Casimir forces and the role of surface modes

I. Pirozhenko¹ and A. Lambrecht²

¹*Bogoliubov Laboratory of Theoretical Physics, JINR, 141980 Dubna, Russia*

²*Laboratoire Kastler Brossel, CNRS, ENS,
UPMC - Campus Jussieu case 74, 75252 Paris, France*

(Dated: October 30, 2018)

Abstract

The Casimir repulsion between a metal and a dielectric suspended in a liquid has been thoroughly studied in recent experiments. In the present paper we consider surface modes in three layered systems modeled by dielectric functions guaranteeing repulsion. It is shown that surface modes play a decisive role in this phenomenon at short separations. For a toy plasma model we find the contribution of the surface modes at all distances.

I. INTRODUCTION

The existence of repulsive Casimir forces follows straightforwardly from the Lifshitz theory [1] for a special choice of the materials. The phenomenon has been discussed in several theoretical papers [3, 4, 5, 6, 7] mainly for materials with nonunit magnetic permeability. Recent advances in the design of metamaterials [8] demonstrating nontrivial magnetic permeability at optical frequencies stimulated experiments seeking after the Casimir repulsion. Though some experimental groups have reported noticeable decrease of the attraction [9] in the presence of metamaterials, to our knowledge, nobody has succeeded so far in reversing the sign of the force.

The repulsive Casimir forces between purely dielectric materials now appear to be more promising for observation and might turn out useful for nanomechanical systems. There repulsion is achieved by filling the space between the bodies with a medium with a precisely chosen dielectric permittivity.

It was experimentally shown [10, 11, 12] for short separations (<50 nm) that repulsive van der Waals forces between specially chosen dielectrics with intervening liquids of low-polarity (eg. cyclohexane, ethanol, or bromobenzene) agree with theoretical predictions of the Lifshitz theory including the retardation contribution. The repulsive Casimir forces at large separations up to several hundred nanometers have not been experimentally studied until very recently [13, 14, 15, 16, 18]

The setup is the following. Two surfaces '1' and '3' with dielectric permittivities ε_1 and ε_3 are separated by a gap filled by medium '2' with dielectric permittivity ε_2 . In recent experiments or proposals medium '2' is a liquid, ethanol [16, 17] or bromobenzene [18] while the two surfaces are made of silica and gold. In order to obtain a repulsive force the respective dielectric functions have to satisfy the relation

$$\varepsilon_1(i\omega) < \varepsilon_2(i\omega) < \varepsilon_3(i\omega). \quad (1)$$

in the frequency range relevant for the force measurement.

The Casimir force is given by [1, 2]

$$F(L) = -\frac{\hbar}{2\pi^2} \sum_{\rho} \int_0^{\infty} dk k \int_0^{\infty} d\omega \kappa_2 \frac{r_{12}^{\rho} r_{32}^{\rho}}{\exp(2\kappa_2 L) - r_{12}^{\rho} r_{23}^{\rho}}. \quad (2)$$

Here L is the width of the gap between the plates; $r_{i2}^\rho(i\omega, \kappa)$, $\rho = TE, TM$, are the reflection coefficients at imaginary frequencies for the surfaces facing the medium '2'

$$r_{i2}^{TM}(i\omega) = \frac{\varepsilon_2 \kappa_i - \varepsilon_i \kappa_2}{\varepsilon_2 \kappa_i + \varepsilon_i \kappa_2}, \quad r_{i2}^{TE}(i\omega) = -\frac{\kappa_i - \kappa_2}{\kappa_i + \kappa_2}, \quad (3)$$

with $\kappa_j(i\omega) = \sqrt{k^2 + \varepsilon_j(i\omega)\omega^2/c^2}$, $j = 1, 2, 3$.

In the present system the Casimir force is repulsive. Indeed, at short distances, $L \ll \lambda_{p,i}$, the force is approximated by $F \approx -H_{123}/3L^3$. Its magnitude and sign is defined by the non-retarded Hamaker constant [19]

$$H_{123} = \frac{3\hbar}{8\pi^2} \int_0^\infty d\omega \sum_{n=1}^\infty \frac{(\Delta_{12}[i\omega] \Delta_{32}[i\omega])^n}{n^3}. \quad (4)$$

with $\Delta_{j2} = (\varepsilon_2(i\omega) - \varepsilon_j(i\omega))/(\varepsilon_2(i\omega) + \varepsilon_j(i\omega))$. Under the condition (1) the Hamaker constants are negative [10, 16] and the force is repulsive.

At long distances $L \gg \lambda_{p,i}$, where the largest contribution to the force comes from small frequencies and small wave vectors κ the reflection coefficients tend to their the static values

$$r_{j2}^{TE}, r_{j2}^{TM} \approx \lim_{\omega \rightarrow 0} \frac{\sqrt{\varepsilon_2(i\omega)} - \sqrt{\varepsilon_j(i\omega)}}{\sqrt{\varepsilon_2(i\omega)} + \sqrt{\varepsilon_j(i\omega)}}. \quad j = 1, 3. \quad (5)$$

Plugging them into (2) one gets a rough estimation of the force at large plates' separations [20]. It is easy to check numerically that if the materials obey (1), especially at low frequencies, the force is repulsive in the long distance limit. These considerations help to choose the materials for the devices based on repulsive Casimir forces [13, 18]. However the origin of this repulsion itself is not quite clear.

In the following we will consider this question in relation with surface modes. The electromagnetic quantum fluctuations which give rise to the Casimir effect obey the Maxwell equations. The corresponding boundary-value problem has two types of solutions: the propagative waves, which will be called photonic modes in the following, and the waves living on the interfaces and exponentially decaying outwards. These surface modes exist only in the TM polarization. Further on we call them surface plasmons or polaritons depending on the model which describes the material. The term "plasmon" is reserved for the plasma model. The expression (2) comprises the contributions from both propagative and surface modes. The present paper pursues their respective roles in the Casimir repulsion by considering a model system consisting of three layers of dielectric material the plasma frequencies of which

are chosen such that condition 1 is fulfilled. Section II and III describe the definition of the surface modes and their contribution to the Casimir energy. In section IV we perform a calculation of the repulsive Casimir force for the recent experiment [18] where we use as dielectric functions the two oscillator model for the silica surface and the bromobenzene liquid filling the gap. The second surface is covered with gold for which we use the Drude model as dielectric response. A comparison between this calculation and the predictions of our model system allows to define the limitations of the latter. The paper finishes with some conclusive remarks in section V.

We will assume that the dielectric properties of the liquid do not change as its layer becomes thicker or thinner. We will not consider the hydrodynamics of this system either. Of course, a body moving in a liquid due to the Casimir attraction or repulsion experiences drag force, which depends on the velocity. This hydrodynamic force should be taken into account in the experiments. Luckily it does not depend on the reason of the movement, and may be estimated separately [14, 15, 18].

II. THE INTERACTION OF THE SURFACE PLASMONS

Let us first formulate the interaction of the surface modes to understand the nature of Casimir repulsion. For simplicity we consider materials described by plasma model, $\varepsilon_i = 1 - \omega_{pi}^2/\omega^2$, $i = 1, 3$, where ω_{pi} is the material's plasma frequency. The frequency of the single surface plasmon living on the interface of medium i , $i = 1, 3$, with medium '2' is given by

$$\omega_{i2}^{sp} = \frac{1}{\sqrt{2}} \left[2k^2 c^2 + \omega_{p2}^2 + \omega_{pi}^2 - \sqrt{4k^4 c^4 + (\omega_{p2}^2 - \omega_{pi}^2)^2} \right]^{\frac{1}{2}} \quad (6)$$

When $k \rightarrow 0$ the single surface plasmon frequency tends to ω_{p2} , provided $\omega_{pi}/\omega_{p2} < 1$, otherwise it approaches ω_{pi} . In the limit $k \rightarrow \infty$ it tends to $\sqrt{\omega_{pi}^2 + \omega_{p2}^2}/\sqrt{2}$, $i = 1, 3$.

The surface modes evanescent in the direction of the gap between the plates are coupled through the cavity. Their frequencies are defined by the equation

$$\prod_{i=1,3} \frac{\varepsilon_2 q_i + \varepsilon_i q_2}{\varepsilon_2 q_i - \varepsilon_i q_2} = e^{-2 q_2 L}, \quad (7)$$

with $q_i = \sqrt{k^2 - \varepsilon_i \omega^2/c^2}$. Let us compare the behavior of the solutions of Eq. (7) in two cases which result in opposite signs of the Casimir force. Fig.1 shows the plasmon modes inside

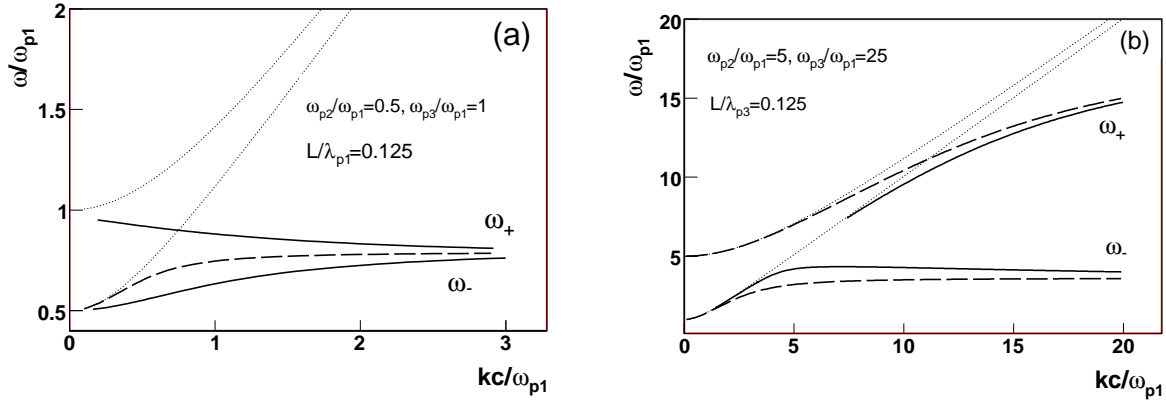


FIG. 1: The plasmon modes in two set-ups: (a) $\omega_{p2} < \omega_{p1}, \omega_{p3}$ (attractive Casimir force), (b) $\omega_{p1} < \omega_{p2} < \omega_{p3}$ (repulsive Casimir force). The solid lines correspond to coupled symmetric and antisymmetric plasmons. The dashed lines show the single surface plasmons living on the interfaces 1-2 and 2-3. The dotted lines mark the boundaries between propagative and evanescent sectors.

the "sandwich" (a) $\omega_{p2} < \omega_{p1}, \omega_{p3}$ (attractive Casimir force), (b) $\omega_{p1} < \omega_{p2} < \omega_{p3}$ (repulsive Casimir force). The coupled plasmon modes are plotted as solid lines. The dashed lines correspond to the plasmons living on the single interfaces. Situation (a) corresponds to well known case where the gap in-between the two plates is filled with vacuum fluctuations ($\omega_{p2} = 0$). It has been studied in detail in the papers [22, 23]. For the sake of comparison with case (b) let us briefly recall the results. Fig.1a shows the solutions of equation (7) when $\alpha \equiv \omega_{p2}/\omega_{p1} = 0.5$, $\beta \equiv \omega_{p3}/\omega_{p1} = 1$ (equal slabs interlaid with material having $\omega_{p,2}$). The dotted lines starting from $\omega/\omega_{p1} = \alpha$ and β separate the propagative and evanescent sectors respectively in the gap and in the slabs. We denote the solutions of (7) by ω_{\pm} , where ω_{+} is usually referred to as antisymmetric plasmon and ω_{-} as symmetric plasmon. The latter one lies entirely in the evanescent sector, $k^2 - \omega^2/c^2 + \omega_{p2}^2/c^2 > 0$. In contrast, the antisymmetric plasmon ω_{+} penetrates into the propagative sector if $k < p_{+}$,

$$p_{+} = \frac{\omega_{p1}}{c} \left\{ \frac{\beta^2 + \frac{\sqrt{\beta^2 - \alpha^2}}{\sqrt{1 - \alpha^2}} + \alpha^2 \sqrt{\beta^2 - \alpha^2} \Lambda}{1 + \frac{\sqrt{\beta^2 - \alpha^2}}{\sqrt{1 - \alpha^2}} + \sqrt{\beta^2 - \alpha^2} \Lambda} - \alpha^2 \right\}^{\frac{1}{2}}, \quad (8)$$

where $\Lambda = L\omega_{p1}/c$ is the dimensionless distance. The coupled plasmons ω_{\pm} surround the single surface plasmon solution ω^{sp} , and $\omega_{+}|_{k \rightarrow 0} = \omega_{p1}$, $\omega_{-}|_{k \rightarrow 0} = \omega_{p2}$. At large wave vectors $\omega_{-} \rightarrow \omega_{12}^{sp}$, $\omega_{+} \rightarrow \omega_{32}^{sp}$. For equal slabs, meaning $\beta = 1$, these limits coincide (dashed line).

The modes which are evanescent in the gap are evanescent within the slabs as well, because on Fig.1a the borderline between the evanescent and the propagative sectors in the gap lies below the corresponding borderline for the slabs.

Fig.1b shows just the opposite situation. The dotted lines starting from $\omega/\omega_{p1} = 1$ and α separate the propagative and evanescent sectors respectively in the gap and in the slab with ω_{p1} . Now the borderline between the two sectors referring to the gap lies above the one corresponding to the slab. In the area between these curves the equation (7) has no real solutions as $q_2^2, q_3^2 > 0$, but $q_1^2 < 0$. Solving (7) with $k^2 - \omega^2/c^2 + \omega_{p2}^2/c^2 \rightarrow 0$, one finds that the mode ω_+ exists for $k > k_+$,

$$k_+ = \frac{\omega_{p1}}{c} \left[\frac{\alpha^2 + \beta^2 f}{1 + f} - 1 \right]^{\frac{1}{2}}, \quad (9)$$

$$f = \frac{\sqrt{\alpha^2 - 1}}{\sqrt{\beta^2 - 1}} \tanh(\Lambda \sqrt{\alpha^2 - 1}).$$

The coupled plasmons ω_{\pm} lie inside the area enveloped by the single surface plasmon solutions ω_{32}^{sp} and ω_{12}^{sp} defined by (6), and $\omega_-|_{k \rightarrow 0} = \omega_{p1}$, $\omega_+|_{k \rightarrow 0} = \omega_{p2}$.

III. THE VACUUM ENERGY OF THE SURFACE MODES

In the following we will concentrate on the Casimir energy contribution of surface modes in the case of a repulsive force. The renormalized vacuum energy of the interacting surface plasmons living on the plane mirrors is formally given by

$$E^{sp} = \frac{\hbar}{2} \sum_{\sigma} \int_{k(\sigma)}^{\infty} \frac{dk k}{2\pi} [\omega_{\sigma}]_{L \rightarrow \infty}^L, \quad \sigma = \pm, \quad (10)$$

where $\lim_{L \rightarrow \infty} \omega_+ = \omega_{12}^{sp}$, $\lim_{L \rightarrow \infty} \omega_- = \omega_{32}^{sp}$, $k_- = 0$, and k_+ is defined by (9).

To calculate the surface plasmon energy, we first introduce the dimensionless variables $K = kL$, $\Omega = \omega L/c$, and $\Omega_{p1} \equiv \Lambda$, $\Omega_{p2} = \alpha\Lambda$, $\Omega_{p3} = \beta\Lambda$ in (7,10)

$$E^{sp} = \frac{\hbar c}{4\pi L^3} \left\{ \int_{K_+}^{\infty} dK K (\Omega_+ - \Omega_{12}^{sp}) + \int_0^{\infty} dK K (\Omega_- - \Omega_{32}^{sp}) \right\}. \quad (11)$$

Then we change the integration variable in (11), $K \rightarrow Q = \sqrt{K^2 - \Omega^2}$ and write the

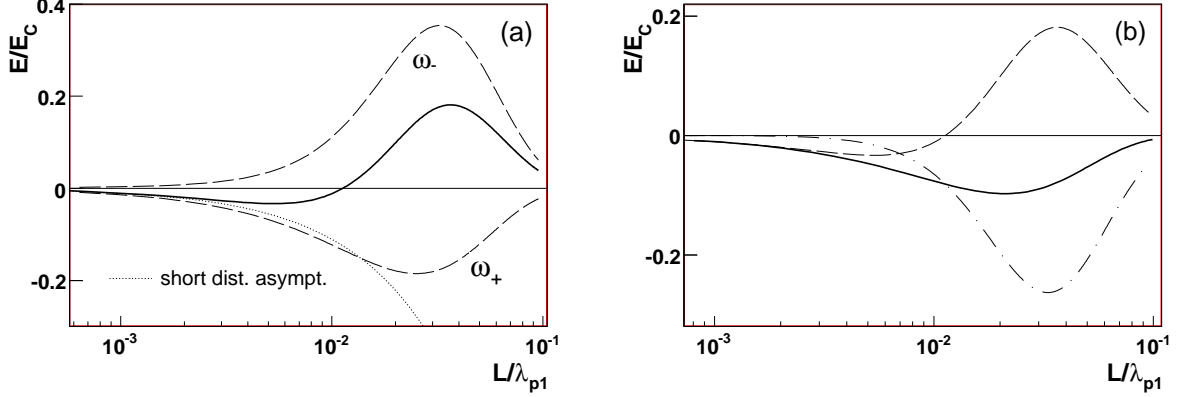


FIG. 2: The normalized vacuum energy: (a) symmetric plasmon ω_- (dashed line), antisymmetric plasmon ω_+ (dash-dotted line), sum of both (solid line); (b) plasmon energy (dashed line), photon energy (dash-dotted line), total Casimir energy (solid line). $\omega_{p2}/\omega_{p1} = 5, \omega_{p3}/\omega_{p1} = 25$.

renormalized energies of the symmetric and antisymmetric plasmons as

$$E^{sp} = \frac{\hbar c}{4\pi L^3} \left\{ \frac{1}{2} \int_{-\Lambda^2}^{\infty} dQ^2 \{ \Omega_- + \Omega_+ - \Omega_{12}^{sp} - \Omega_{23}^{sp} \} - \frac{1}{2} \int_X^{-\Lambda^2} dQ^2 \Omega_{12}^{sp} + \frac{1}{3} (\Omega_+^3 - \Omega_{12}^3)|_{K_{(+)}}^{\infty} \right\}, \quad (12)$$

where $X = K_+^2 - \Omega_{12}^2(K_+)$.

The numerical results for the plasmon energy are given in Fig.2(a). The distance is normalized by the largest plasma wavelength in the system, $\lambda_{p1} = 2\pi c/\omega_{p1}$. The plot shows the reduction factor which is the ratio of the plasmon vacuum energy and the Casimir energy of perfectly conducting plates, $E_C = -\hbar c\pi^2/720L^3$. As the Casimir force between perfectly conducting plates is attractive, a negative or positive reduction factor corresponds to repulsion or attraction respectively. For the energies, the arguments goes in the opposite way. The energy of the antisymmetric plasmon ω_+ is positive, corresponding to repulsion with a negative reduction factor, while the energy of the symmetric plasmon ω_- is negative yielding attraction and thus a positive reduction factor. The antisymmetric plasmon dominates at short distances, while the symmetric plasmon makes decisive contribution at larger separations. Thus the total plasmon interaction is repulsive at short separations and attractive at medium and long distances. Here we estimate the length scale with respect to λ_{p1} .

In [22, 23], it was shown that for two plates separated by vacuum the attractive Casimir energy is a result of cancelations between plasmon and photon contributions at all distances. Moreover the plasmon and photon energies have different signs and decrease more slowly with distance ($\sim L^{-5/2}$) than the total energy ($\sim L^{-3}$).

Fig.2(b) shows the reduction factor for the total Casimir energy when condition (1) is met. Clearly it is negative at all distances corresponding to a repulsive Casimir interaction. It comes out as the sum of negative photon contribution and the plasmon contribution, plotted in Fig.2(a). The plasmon contribution dominates at short separations. At medium and long distances the photon contribution prevails assuring repulsion. At distances large with respect to λ_{p1} the energy decreases as $E \sim \text{Ei}(1, 2\alpha\Lambda)$, $\Lambda = 2\pi L/\lambda_{p1}$. The decrease is much steeper than in any set-up yielding attraction.

The attraction of the surface plasmons at short ranges explains the sign and the magnitude of the Casimir force between plates separated by vacuum (or any material with $\omega_{p2} < \omega_{p1}, \omega_{p3}$). In the following we will show that under the condition (1) the surface plasmons produce a repulsive contribution at short distances.

The equation for the interacting surface plasmons may be solved explicitly for large wave vectors which correspond to short distances:

$$(\omega_{\pm})^2 = \frac{1}{4} \{ 2\omega_{p,2}^2 + \omega_{p,1}^2 + \omega_{p,3}^2 \mp [(\omega_{p,1}^2 - \omega_{p,3}^2)^2 + 4(\omega_{p,1}^2 - \omega_{p,2}^2)(\omega_{p,3}^2 - \omega_{p,2}^2)e^{-2|k|L}]^{1/2} \}. \quad (13)$$

Then the vacuum energy is

$$E_{as}^{sp} = \frac{\hbar\omega_{p,1}}{32\pi L^2} Y(\alpha, \beta) \quad (14)$$

where

$$Y = \int_0^{\infty} dk k \{ \psi_+ + \psi_- - \sqrt{2} [(1 + \alpha^2)^{\frac{1}{2}} + (\beta^2 + \alpha^2)^{\frac{1}{2}}] \},$$

$$\psi_{\pm} = \left\{ 2\alpha^2 + 1 + \beta^2 \mp [(1 - \beta^2)^2 + 4(1 - \alpha^2)(\beta^2 - \alpha^2)e^{-k}]^{\frac{1}{2}} \right\}^{\frac{1}{2}}. \quad (15)$$

If at large frequencies condition (1) is satisfied, then $E_{as}^{sp} > 0$ yielding repulsion. The simplest particular case is $\beta = \alpha^2 > 1$ ($\omega_{p,2}/\omega_{p,1} = \omega_{p,3}/\omega_{p,2}$) corresponding to equal ratios between the plasma frequencies. For large α , $\psi(\alpha \rightarrow \infty) \rightarrow 0.67\alpha$. If $\alpha = 1 + \delta$, $Y(\delta \rightarrow 0) \approx \delta^2/2$. For

example, $Y(1.1) = 0.00497$. Thus, the vacuum energy of the interacting surface plasmons is positive corresponding to repulsion.

IV. REPULSIVE CASIMIR FORCE USING THE DIELECTRIC RESPONSE OF THE MATERIALS

Let us now compare the repulsive force due to the interaction of the surface modes obtained in the plasma model with the corresponding total Casimir force calculated according to the zero temperature Lifshitz formula (2). On Fig.3 we plot the force (2) normalized by the Casimir force between perfect conductors as a function of the dimensionless distance L/λ_{p1} , $\lambda_{p1} = 2\pi c/\omega_{p,1}$. The calculation is done for tree layers with $\varepsilon_i = 1 + \omega_{pi}^2/\omega^2$, $\alpha = \omega_{p2}/\omega_{p1} = 5$, $\beta = \omega_{p3}/\omega_{p1} = 25$ (solid line). At short distances the force coincides with the short distance asymptote of the interacting surface plasmons, $F_{as}^{sp} = -dE_{as}^{sp}/dL$, $F_{as}^{sp}/F_C = -7.38L/\lambda_{p1}$ (dotted line). At long distances ($L \gg \lambda_{p2}$) the force is repulsive and decays much faster than the force between two plates separated by vacuum, $F \sim \exp(-2\omega_{p2}L/c)/L$, where ω_{p2} is the plasma frequency of the material filling the gap. This behavior is explained by the divergence of ε_2 for $\omega \rightarrow 0$ within the plasma model. If dielectric function of the intermediate material '2' is finite at low frequencies, the reduction factor saturates at large distances.

An example of a more realistic set-up is the system Silica-Bromobenzene-Gold. Repulsive dispersion forces in a similar system were measured by [10] at short distances, the results appeared to be consistent with the calculated non-retarded Hamaker constants. Precisely the same system was studied in a recent experiment [18] at separations from 20 nm to several hundred nanometers. Here we do not consider separations larger than 300 nm, so that we need not to account for temperature corrections. In the following we first calculate the reduction factor applying the zero temperature Lifshitz formula (2) with the materials described by Drude and Lorentz models.

For gold $\varepsilon_{Au}(i\omega) = 1 + \omega_{Au}^2/[\omega(\gamma + \omega)]$, where $\omega_{Au} = 1.367 \cdot 10^{16}$ rad/s, $\gamma = 5.316 \cdot 10^{13}$ rad/s [2]. To simplify the analysis for bromobenzene and silica we confine ourselves to two oscillators in the standard multiple oscillator model

$$\varepsilon_i(i\omega) = 1 + \frac{C_{IR}^i}{1 + (\omega/\omega_{IR}^i)^2} + \frac{C_{UV}^i}{1 + (\omega/\omega_{UV}^i)^2}, \quad (16)$$

where $i = 1, 2$ and correspond to silica and bromobenzene respectively. The various param-

eters are $C_{IR}^1 = 0.829$, $\omega_{IR}^1 = 0.867 \cdot 10^{14}$ rad/s, $C_{UV}^1 = 1.098$, $\omega_{UV}^1 = 2.034 \cdot 10^{16}$ rad/s [19]; $C_{IR}^2 = 2.967$, $\omega_{IR}^2 = 5.47 \cdot 10^{14}$ rad/s, $C_{UV}^2 = 1.335$, $\omega_{UV}^2 = 1.286 \cdot 10^{16}$ rad/s [10]. With these values of the parameters the condition (1) is satisfied for $\omega < 9 \cdot 10^{15}$ rad/s, where $\varepsilon_{SiO_2} < \varepsilon_{C_6H_5Br} < \varepsilon_{Au}$. For $\omega > 3 \cdot 10^{16}$ rad/s, $\varepsilon_{Au} < \varepsilon_{C_6H_5Br} < \varepsilon_{SiO_2}$. Both regions contribute to repulsion *within the two oscillator model for bromobenzene and silica*. The applicability of this model is discussed in [17, 18].

In the present situation the solutions of (7) are interacting surface polaritons. At close separations realized by a thin layer of bromobenzene, where the decisive contribution to the force comes from large wave vectors and high frequencies, the absorption is negligible, and the models used for the materials are reduced to the plasma model with effective plasma frequency $\omega_{pi}^{eff} = [C_{UV}^i \omega_{UV}^2 + C_{IR}^i \omega_{IR}^2]^{1/2}$, $i = 1, 2$, $\omega_{p3} = \omega_{Au}$. We find $\omega_{SiO_2}^{eff} = 2.131 \cdot 10^{16}$ rad/c, $\omega_{C_6H_5Br}^{eff} = 1.488 \cdot 10^{16}$ rad/c.

At close separation the surface polaritons turn into surface plasmons, and the formulae (13-15) for the the interacting surface plasmons become valid. But one should keep in mind that they describe correctly only short distance regime. Substituting $\alpha = \omega_{p2}^{eff}/\omega_{p1}^{eff} = 0.698$, $\beta = \omega_{p3}/\omega_{p1}^{eff} = 0.641$, we get $F_{as}^{sp}/F_C = -0.03355 L/\lambda_{p1}^{eff}$, where $\lambda_{p1}^{eff} \equiv \lambda_{SiO_2}^{eff} = 2\pi c/\omega_{p1}^{eff} = 88.44$ nm is the effective plasma wavelength for the composed system. In this regime the reduction factor for the interacting surface modes is negative yielding repulsion. It coincides with the total reduction factor for the force at short distances.

At medium and low frequencies the dielectric functions of the materials are complex, and the calculation of the vacuum energy corresponding to the surface modes is not so straightforward. The total reduction factor for the force is shown as the dashed line in Fig.3. Clearly repulsion sets in for distances of the order of or larger than the effective plasma frequency while the toy model gives repulsion essentially for distances much smaller than that and gives a negligible force for larger distances. In contrast at large distances our calculation using the two oscillator model yields a negative force with a reduction factor which reaches $\eta \approx -0.057$. Within the plasma model the reduction factor decays exponentially, while within the two oscillator model it tends to a constant. This shows that the repulsion at large distances does not have its origin in the interaction between surface modes but stems from the repulsive contribution of propagating modes.

The dotted lines are the short distance plasmon approximations to the model system

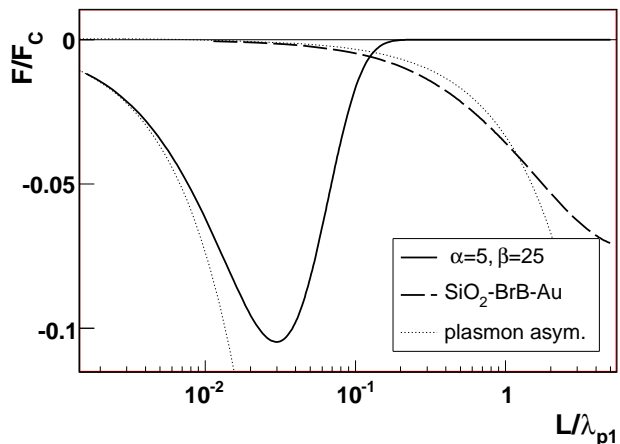


FIG. 3: Reduction factor $\eta_F = F/F_C$ at short plate separations as a function of dimensionless distance $\Lambda = L/\lambda_{p1}$; $\alpha = \omega_{p,3}/\omega_{p,2} = \omega_{p,2}/\omega_{p,1}$. The dotted lines are the respective short distance asymptotes of the surface plasmon interaction. $\alpha = \omega_{p,3}/\omega_{p,2} = \omega_{p,2}/\omega_{p,1}$. For the system $\text{SiO}_2\text{-C}_6\text{H}_5\text{Br-Au}$ $\lambda_{p1} = 2\pi c/\omega_{p,\text{SiO}_2}^{\text{eff}} = 88.44\text{nm}$.

and for the realistic dielectric response functions. For the latter the plasmon approximation turns out to be valid for distances up to twice the effective plasma wavelength, that is about 170 nm. Indeed, the present calculation does not pretend to be a precise description of the recent experiment [18], but the system $\text{Au} - \text{C}_6\text{H}_5\text{Br} - \text{SiO}_2$ is used as an illustration.

The calculation of the Casimir force at zero temperature for the solid-liquid-solid system using measured dielectric functions of all involved materials for the wavelength range from millimeters down to subnanometers was carried out in [24], which was submitted simultaneously to the present paper.

V. CONCLUSION

In the present paper we have studied the Casimir force in the systems which meet the condition (1). The magnitude of the force in the present setup is small. For example, in the system $\text{SiO}_2 - \text{C}_6\text{H}_5\text{Br} - \text{Au}$, with the 150 nm layer of bromobenzene, it is only about 5% of the force between gold covered plates in vacuum.

From previous studies [7, 21, 22, 23] we remember that when two plates in vacuum form a cavity, the total energy of the coupled surface modes is negative, corresponding to attraction.

We have shown that within the plasma model the surface modes repel at short distances when the materials satisfy the condition (1). Moreover the Casimir repulsion is then completely due to the repulsion of the surface modes. At medium and long distances the interaction of the surface modes becomes attractive, but the dominating repulsive contribution of the propagative modes leads to a total repulsive force.

Acknowledgments

We acknowledge financial support from the European Contract No. STRP 12142 NANOCASE.

-
- [1] E. M. Lifshitz. *Soviet Phys. JETP*, 2:73, 1956.
 - [2] A. Lambrecht and S. Reynaud. *Eur. Phys. Journ.* **D8**, 309 (2000).
 - [3] T. H. Boyer. *Phys. Rev.* **A 9**, 2078–2084 (1974).
 - [4] O. Kenneth, I. Klich, A. Mann, and M. Revzen. *Phys. Rev. Lett.* **89**, 033001 (2002).
 - [5] C. Henkel and K. Joulain. *Europhys. Lett.* **9(6)**, 929–935 (2005).
 - [6] F.S.S. Rosa, D.A.R. Dalvit, P.W. Milonni . *Phys. Rev. Lett.***100**, 183602 (2008).
 - [7] I. G. Pirozhenko and A. Lambrecht. *Journal Physics A* **41(16)**, 164015 (2008).
 - [8] V.G. Veselago, L. Braginsky, V. Shklover, Ch. Hefner, *J. Comput. Theor. Nanosci.* **3**, N 2, 1 (2006).
 - [9] Chris Binns, Private communication.
 - [10] A. Milling, P. Mulvaney, I. Larson. *J. of Colloid and Interface Science*, **180**, 460-465 (1996).
 - [11] Seung-woo Lee and Wolfgang M. Sigmund. *J. of Colloid and Interface Science*, **243**, 365 - 369 (2001).
 - [12] Seung-woo Lee and Wolfgang M. Sigmund. *Colloids and Surfaces A: Physicochemical and Engineering Aspects*, **204**, 43 - 50 (2002).
 - [13] Alejandro W. Rodriguez, J. N. Munday, J. D. Joannopoulos, Federico Capasso, Diego A. R. Dalvit, and Steven G. Johnson. *Phys. Rev. Lett.* **101**, 190404 (2008).
 - [14] J. N. Munday and Federico Capasso. *Physical Review A* **75**, 060102(R) (2007).

- [15] J. N. Munday, Federico Capasso, V. A. Parsegian and Sergey M. Bezrukov. *Phys. Rev. A* **78**, 032109 (2008).
- [16] Federico Capasso, Jeremy N. Munday, Davide Iannuzzi, and H. B. Chan. *IEEE JOURNAL OF SELECTED TOPICS IN QUANTUM ELECTRONICS*, **13(2)** 400–414 (2007).
- [17] P.J. van Zwol, G. Palasantzas, J. Th. M. De Hosson. Weak dispersive forces between glass-gold macroscopic surfaces in alcohols arXiv:0904.0622 (2009).
- [18] J. N. Munday, F. Capasso, A. Parsegian, *Nature* **457**, 170 (2009).
- [19] Lennart Bergström. *Advances in Colloid and Interface Science* **70**, 125–169, 1997.
- [20] I. Pirozhenko and A. Lambrecht. *Physical Review A* **77** 013811 (2008).
- [21] C. Henkel, K. Joulain, J.-Ph. Mulet, and J.-J. Greffet. *Phys. Rev. A* **69** 023808 (2004).
- [22] F. Intravaia and A. Lambrecht. *Physical Review Letters* **94** 110404 (2005); idem **96** 218902 (2006).
- [23] M. Bordag. *Journal Physics A* **39**, 6173–6186 (2005).
- [24] P.J. van Zwol, G. Palasantzas, J. Th. M. De Hosson. The influence of dielectric properties on van der Waals/Casimir forces in solid-liquid systems arXiv:0905.0889 (2009)